Interfacial magnetoelectric coupling in tricomponent superlattices

Jaekwang Lee, Na Sai,* Tianyi Cai, Qian Niu, and Alexander A. Demkov†
Department of Physics, The University of Texas at Austin, Austin, Texas 78712, USA
(Received 14 December 2009; revised manuscript received 1 April 2010; published 26 April 2010)

Using first-principles density-functional theory, we investigate the interfacial magnetoelectric coupling in a tricomponent superlattice composed of a ferromagnetic metal (FM), ferroelectric (FE), and normal metal. Using Fe/FE/Pt as a model system, we show that a net and cumulative interfacial magnetization is induced in the FM metal near the FM/FE interface. A careful analysis of the magnetic moments in Fe reveals that the interfacial magnetization is a consequence of a complex interplay of interfacial charge transfer, chemical bonding, and spin-dependent electrostatic screening. The last effect is linear in the FE polarization, is switchable upon its reversal, and yields a substantial interfacial magnetoelectric coupling.

DOI: 10.1103/PhysRevB.81.144425 PACS number(s): 75.85.+t, 75.70.Cn, 77.84.−s, 73.20.At

Materials with coupled magnetic and electric degrees of freedom are classified as magnetoelectrics (MEs). A strong magnetoelectric coupling enables control of magnetism by the electric field or vice versa, and hence has a strong appeal for emerging device applications.[1–4] A linear coupling between these two degrees of freedom involves breaking both space and time-reversal symmetries and is therefore of fundamental interest. Multiferroic oxides in which simultaneous ferroelectric (FE) and magnetic orders exist form a class of promising magnetoelectric materials. However, many single phase multiferroics have rather limited application either because of their low Curie temperature or weak coupling.

Heterointerfaces have proven to be ideal for controlling and manipulating electrical charges and spins in solid-state devices. Recently, efforts have focused on the so-called "interfacial magnetoelectricity" in which a magnetoelectric coupling arises at a ferromagnetic metal (FM)/dielectric (or ferroelectric) interface.[5–12] A ferroelectric or a dielectric (upon the application of an electric field) can induce free charges near the interface within a ferromagnetic metal. These screening charges are spin dependent in the ferromagnet, and thus in turn yield an additional magnetization that exists only within a nanometer near the interface. In contrast to the intrinsic coupling in multiferroic oxides, this effect can be viewed as an extrinsic magnetoelectric effect and may offer an alternative to a single phase multiferroic in providing the robust room-temperature ME effect.

In this paper we explore "tricomponent" FM/FE/normal-metal (NM) superlattices consisting of alternating layers of a ferromagnetic metal, ferroelectric, and normal metal as depicted in Fig. 1. Unlike the symmetric heterostructure,[6,7,10–12] the broken inversion symmetry in an asymmetric superlattice permits a leading magnetoelectric coupling in the free-energy expansion that is linear in the electric polarization of the FE,[8] i.e., $\propto PM^2$, and hence can be electrically controlled. Moreover, since the induced magnetization only occurs at the FM/FE interface, the overall induced magnetization does not cancel as in the symmetric structure[6] and can cumulate in a superlattice to achieve a large macroscopic magnetization.

Using density-functional theory (DFT), we demonstrate this effect using Fe/FE/Pt superlattices, where for FE we use $BaTiO_3$ (BTO) and $PbTiO_3$ (PTO) as two examples. PTO and BTO are two prototypical FEs with robust room-temperature polarization. Their significant difference in polarization allows us to investigate the polarization dependence of the ME coupling effect. A rather complex picture emerges as a result of a detailed electronic structure analysis. The interface magnetization is controlled by the interplay of quite different physical effects including electrostatic screening, contact potential difference, formation of the Fe-O chemical bonds, metal induced gap states, and subtle chemical differences resulting from the polarization switching. The electrostatic effect is approximately linear in the FE polarization and switchable upon the reversal of the polarization, in agreement with the analytical model.[8] The overall magnetoelectric coupling we find in these systems is remarkably large compared to many other existing composite structures that have been reported so far.[13,14]

We use DFT within the local-density approximation (LDA) as implemented in the VASP code and projector augmented-wave pseudopotentials.[15] We apply a plane-wave cutoff energy of 600 eV and the $8\times8\times8$ and $8\times8\times2$ k-point meshes for the Brillouin-zone integration for the bulk and superlattice, respectively. Calculations of the lattice parameter in the tetragonal phase yield 3.86 Å, $c/a=1.04$ for PTO and 3.95 Å, $c/a=1.01$ for BTO. The lattice constants are about 1.5% less than the experimental values of 3.904 and 3.994 Å,[16] as is typical for DFT-LDA calculations. For two metal electrodes, bcc Fe and fcc Pt, we find lattice parameters of 3.904 Å and 3.901 Å, respectively, to be compared to the experimental values of 4.05 and 3.92 Å. We terminate the FEs with TiO_2 planes and place the Fe and Pt atoms atop oxygen. Asymmetric termination[17] of the FE ca-

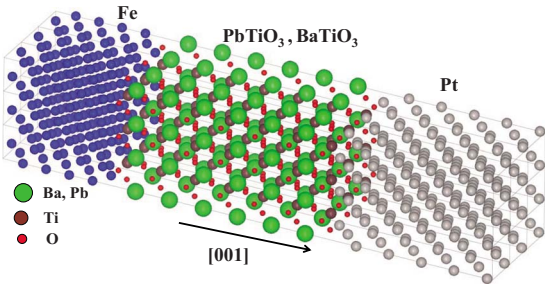

FIG. 1. (Color online) Schematics of the tricomponent superlattices which consist of alternatively stacked ferromagnetic metal (Fe), ferroelectric, and normal metal (Pt).

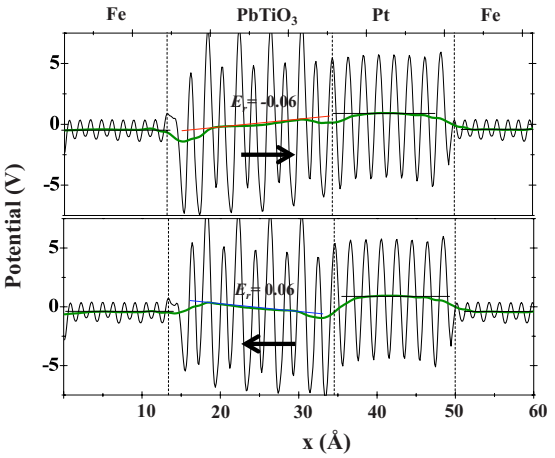

FIG. 2. (Color online) The planar (thin gray curve) and macroscopically averaged potential (thick green curve) as a function of distance along the [001] direction for the fully relaxed $(Fe)_{11}(PbTiO_3)_9(Pt)_8$ superlattice. The straight line in PTO marks the residual field in the PTO unit cells, where a magnitude of ± 0.06 eV/Å is calculated. The arrows mark the direction of the FE polarization in $PbTiO_3$.

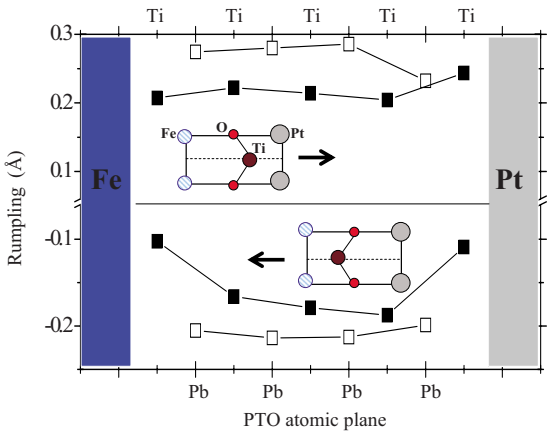

FIG. 3. (Color online) The rumpling parameter for each $PbTiO_3$ atomic plane in the $(Fe)_{11}/(PbTiO_3)_9/(Pt)_8$ superlattice. The insets illustrate the relative position of the interfacial TiO_2 plane with respect to the adjacent Fe and Pt atoms. The arrows mark the direction of the polarization in $PbTiO_3$.

pacitor has not been considered in the present calculations. We have modeled two superlattices, $(Fe)_{11}(PTO)_9(Pt)_8$ and $(Fe)_9(BTO)_{13}(Pt)_{10}$ (the subscripts indicate the number of atomic layers). We start with an out-of-plane FE displacements calculated for the bulk phase and fully relax the structure until the maximum force is below 10 meV/Å, keeping the in-plane lattice constants fixed to the theoretical bulk value.[18] In-plane ferroelectric instability has been ignored because it does not pertain to the magnetoelectric effect in this study. In the BTO superlattice, the lattice constant constraint leads to in-plane tensile strain of about 1% and 1.2% in Fe and Pt, respectively, and in the case of PTO compressive strain of about −1% and −0.9% in Fe and Pt, respectively.[19]

We start with discussing the $Fe/PbTiO_3/Pt$ superlattice. The macroscopically averaged electrostatic potentials of the relaxed supercell for two opposite directions of FE polarization are shown in Fig. 2. Within a standard FE capacitor model,[20,21] the depolarizing field in the ferroelectric film is proportional to $8\pi P\lambda_M/d_{\mathrm{FE}}$, where λ_M and d_{FE} are the screening length of the metal electrodes and the thickness of the FE film. Within this model, the depolarizing field vanishes only if $\lambda_M \to 0$, in which case the surface polarization charges are fully compensated by the free charges in the metal. Figure 2 shows a residual depolarizing field of about 0.06 V/Å in the PTO layers that points in the direction opposite of polarization, indicating incomplete screening by the metallic electrodes.[22] The residual field in the PTO superlattice is about 17% of the depolarizing field calculated for an isolated PTO film. This ratio is comparable to $2\lambda_M/d_{\mathrm{PTO}} \sim 13\%$, where the FE thickness d_{PTO} is 16 Å and screening length of Fe λ_M is about 1 Å.[23]

Using the Born effective charges[24] and ionic displacements relative to the ideal positions, we estimate the polarization of the central unit cell to be about 75 and 70 $\mu C/cm^2$ when the polarization points toward Pt and Fe, respectively. These values are slightly reduced compared to the calculated bulk value of 84 $\mu C/cm^2$. (For the $BaTiO_3$ based structure, we have found 20 and 18 $\mu C/cm^2$ for the respective polarization, whereas the bulk value is 25 $\mu C/cm^2$.) Figure 3 shows the rumpling parameter, defined as the relative displacement between the cations and oxygen ions for each atomic plane along the stacking direction of the PTO superlattice. The amplitudes of the interfacial rumpling are roughly 0.1 Å higher when the polarization points toward Pt than when it points toward Fe. The higher amplitude in the former case is consistent with that observed in $Pt/PbTiO_3/Pt$ (Ref. 25) and can be most likely attributed to the formation of metallic bonding between Pt and Ti at the Pt/PTO interface and the Fe-O bonding at the Fe/PTO interface.

Assuming the FE layers stay in a single-domain state, the ferroelectric polarization then terminates at a FE/metal interface, and induces screening charges in the metal. The total screening induced charge density satisfies the Poisson equation

$$\frac{d^2V_c(x)}{d^2x} = -(e/\epsilon_0)[\delta n^{\uparrow}(x) + \delta n^{\downarrow}(x)], \tag{1}$$

where V_c is the Coulomb screening potential in the metal and δn^{σ} is the screening induced charge density of spin $\sigma = \uparrow, \downarrow$. If the metal is a FM, then the induced charges are spin dependent due to the exchange interactions and a local magnetization can be induced at the interface. The local induced magnetization and the Coulomb screening potential at a FM/dielectric[5] or FM/FE interface[8] can be related through

$$\delta n^{\uparrow}(x) - \delta n^{\downarrow}(x) = -\frac{M_0}{1 + JN_0} eV_c(x), \tag{2}$$

where M_0 and N_0 are the spontaneous magnetization and the total density of states (DOS), and J is the exchange splitting in the FM. Thus the induced magnetization switches sign when the orientation of the FE polarization switches.

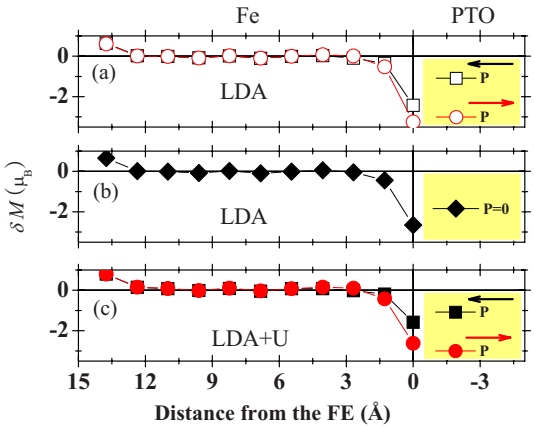

FIG. 4. (Color online) The layer by layer magnetic moment changes relative to the bulk of two Fe atoms per lateral unit cell of the $(Fe)_{11}/(PbTiO_3)_9/(Pt)_8$ superlattice. The PTO is in a (a) ferroelectric phase where the FE polarization directions are marked by the arrows and (b) paraelectric phase. (c) The magnetic moment changes calculated within LDA+U (where U=8 eV).

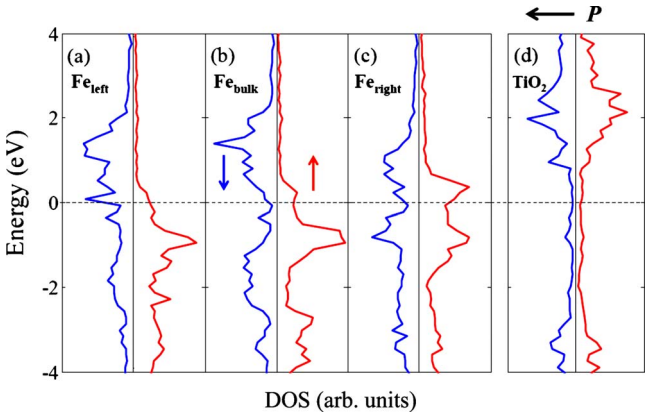

FIG. 5. (Color online) The projected DOS (PDOS) of interfacial Fe atoms in the Pt/PTO/Fe superlattice at the (a) Pt/Fe interface, (b) Fe bulk region, and (c) Fe/PTO interface. Panel (d) shows the PDOS of the interfacial TiO_2 layer in PTO. The up and down arrows represent the spin-majority and spin-minority channels, respectively.

To calculate the interfacially induced charge density of Fe due to the spin-dependent screening, we project the DOS of the $Fe/PbTiO_3/Pt$ superlattice onto each atomic layer of Fe parallel to the interface. By integrating the DOS below the Fermi level separately for the spin-up and spin-down components, we obtain the layer by layer magnetization densities $n^{\uparrow}(x)-n^{\downarrow}(x)$ in the Fe unit cells. In Fig. 4(a), we plot the change in the layer by layer magnetization density with respect to the bulk value ($\sim 4\mu_B$/lateral unit cell counting two Fe atoms) for two opposite polarization directions in PTO. The total magnetization of Fe is significantly suppressed with respect to the bulk at the Fe/PTO interface and slightly enhanced at the Pt/Fe interface. To understand this behavior, we plot $\delta M(x)$ of Fe when PTO is in a paraelectric phase, i.e., P=0, in Fig. 4(b) for comparison. It is clear that similar changes in the magnetic moment in Fe at both interfaces exist even in the absence of the FE polarization. We start by explaining this effect.

The reduction in the iron's magnetic moment at the Fe/oxide interface is caused by charge transfer from Fe to the oxide resulting from several mechanisms. In Fig. 5, we show the DOS of Fe at both interfaces and compare them to that in the interior bulk region. At the Fe/PTO interface as shown in Fig. 5(c), the majority-spin state at the Fermi level dominates, same as in bulk Fe. Thus losing charge from Fe to the oxide suppresses the majority spin more than the minority and leads to a reduction in the magnetic moment of Fe. The outflow of charge from Fe into the oxide is caused by two effects. First and the larger of the two is the formation of Fe-O bonds at the interface. Electronegative oxygen pulls the charge away from Fe. Second effect is filling of the so-called metal induced gap states that are clearly seen in Fig. 5(d). This is universal for any metal/insulator interface when the metal Fermi level happens to be in the gap of the insulator. At the Fe/Pt interface, on the other hand, the density of states of Fe at the Fermi level is reversed with respect to the bulk as can be seen in Figs. 5(a) and 5(b). Thus charge transfer from Fe into Pt due to the work function difference (the work function of Fe is 2 V less than Pt) results in losing more minority spins and therefore increases the magnetic moment in Fe. We find a similar effect in our Pt/Fe bilayer calculation. The comparison with the P=0 case corroborates that the large moment change relative to the bulk is independent of polarization. In the following, we will remove this effect from the polarization-dependent induced magnetization.

Before proceeding, we make two relevant comments. The charge transfer from Fe to oxide is exacerbated by the reduction in the PTO band gap to about 2 eV within the LDA, compared to the experimental gap of 3.5 eV. By applying a Hubbard-U correction to Ti 3d states, the band gap of the oxide is opened up[26] and the overall magnetic moment reduction has been reduced as shown in Fig. 4(c). However, the polarization dependence of the induced magnetization which is the main focus of the paper qualitatively stays the same. Henceforth we only discuss the results from the LDA calculations. We further note that a recent study[7] of a symmetric $Fe/BaTiO_3/Fe$ junction reported large induced magnetic moments on interfacial Ti atoms, even higher than the induced moments on the interfacial Fe atoms. The authors attributed the moment changes on Ti to a significant hybridization between the 3d orbitals of Ti and Fe at the interface. In contrast to the DOS in Ref. 7, our interfacial Ti d orbitals lie mostly above the Fermi level as shown in Fig. 5(d). Therefore the moment changes on the interfacial Ti atoms are much smaller than those of Fe in our calculation and will be ignored in our study.

To focus on the polarization related changes in magnetization we subtract $\delta M(P=0)$ from $\delta M(\pm P)$ shown in Fig. 4. Thus we obtain the polarization-induced magnetization of Fe near the PTO interface for two opposite FE polarization directions as shown in Fig. 6(a). We include the results from the BTO superlattice as well. In either case, the induced moments decay rapidly as function of distance away from the FM/FE interface and change sign as the FE polarization direction switches. This suggests that if bias is applied to switch the FE polarization, the magnetization becomes electrically controllable as consistent with our model

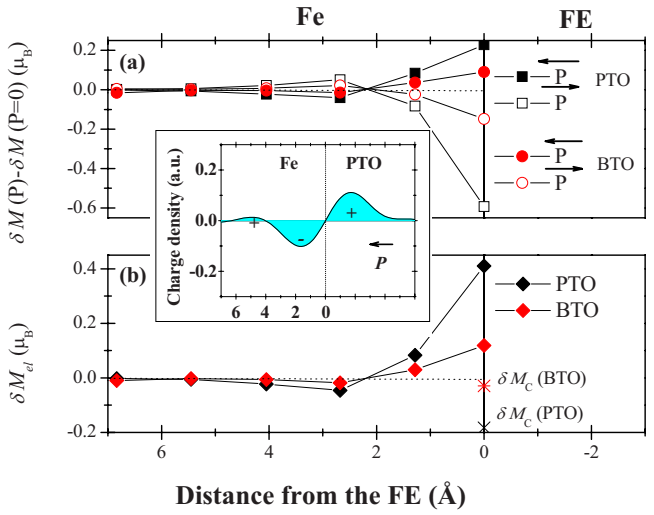

FIG. 6. (Color online) (a) The magnitude of the polarization-induced magnetization for two Fe atoms per lateral unit cell vs distance from the Fe/FE interface for the PTO and BTO based superlattice. Only half of the Fe cell close to the oxide is plotted. (b) The electrostatic screening induced magnetization δM_{el} (diamonds) and the magnetization induced by a chemical component related to polarization switching δM_c (stars). The inset shows the induced charge density near the Fe/PTO interface.

calculation.[8] It is interesting to note that δM, however, does not completely follow an exponential function as typically assumed in screening models. As the distance from the interface increases, the sign of δM oscillates. We attribute this behavior to Fridel-type oscillations in the metal.[27] It is consistent with the induced charge-density distribution (see the inset) calculated from the electrostatic potential near the interface, which also oscillates.

Unlike the rest of the Fe layers, the induced moment on the first interfacial layer of Fe is significantly asymmetric with respect to the direction of the polarization. To explain the asymmetry, we make a reasonable assumption that the total induced magnetization can be decomposed into two separate terms, δM_{el} and δM_c. The first term is related to electrostatic screening which changes sign as the polarization switches and the second term is an additional contribution which is related to the chemical bonding at the interface,

$$\begin{cases} \delta M(+P) = \delta M_{el} + \delta M_{c1} \\ \delta M(-P) = -\delta M_{el} + \delta M_{c2}. \end{cases} \quad (3)$$

Since the opposite polarization directions result in different interfacial atomic configurations (Fe-O-Ti vs Fe-Ti-O as illustrated in Fig. 3 insets), δM_c could be different in these equations. However, in an attempt to separate the effect of the electrostatic screening and chemical bonding, we assume the difference between δM_{c1} and δM_{c2} to be much less than the screening induced moment change and therefore $\delta M_{c1} \approx \delta M_{c2}$. We calculate δM_{el} and δM_c by subtracting and adding $\delta M(+P)$ and $\delta M(-P)$ and plot them in Fig. 6(b). Note that δM_c exists only in the first interfacial layer. The magnitudes of both δM_{el} and δM_c are strongly dependent on the magnitude of the polarization in the FE oxide. For superlattice with thick FE layers where the residual depolarizing field can be neglected, the screening induced interfacial contribution to the magnetization should be even higher. In the PTO and BTO superlattice, the maximum magnitude of the screening induced moment change $\delta M_{el}(x)$ is about $0.4\mu_B$ and $0.13\mu_B$ per surface unit cell, corresponding to a surface spin density of 53 $\mu C/cm^2$ and 14 $\mu C/cm^2$, respectively. The ratio between the two resembles closely the ratio between the calculated polarization of PTO and BTO. Thus the electrostatically induced magnetization is clearly linear in the FE polarization, in agreement with Eqs. (1) and (2). This also suggests that our approximation for δM_c is reasonable. On the other hand, the magnitudes of δM_c are quite different, 0.19 and $0.03\mu_B$, at the Fe/PTO and Fe/BTO interfaces, indicating a different interfacial bonding character between two different FEs with metals.[28]

To estimate the ME coupling, we use the dimensionless ratio[6] between the screening induced magnetization density and bulk electric polarization of the FE, i.e., $\eta = \frac{\delta M_{el}}{P}$. The maximum values of η are estimated to be 0.66 and 0.61 at the Fe/PTO and Fe/BTO interface, respectively, higher than that estimated in Ref. 6 at the $SrRuO_3/BaTiO_3$ interface. For comparison, we also quantify the ME coupling using the definition that is strictly only suitable for bulk materials $\mu_0 \delta M_{el} = \alpha E_c$, where E_c is the coercive field of the FEs and μ_0 is the vacuum permeability. Using a typical value of $E_c \sim 100$ kV/cm, we estimate the maximum interfacial magnetoelectric coefficient α to be 3×10^{-10} G cm^2/V which is of similar order of magnitude as that reported by Duan *et al.*[7] However the ME coupling in our study arises solely from electrostatic screening, in contrast to the dominant contribution from orbital hybridization in Ref. 7. The magnitude of the charge-mediated ME coupling seems comparable to the strain-mediated magnetoelectric susceptibility ($\sim 10^{-2}$ G cm/V or $\sim 10^{-10}$ G cm^2/V in two dimension) observed in $CoFe_2O_4/BiFeO_3$ (Ref. 14) although a theoretical prediction of two orders of magnitude higher (~ 1 G cm/V) has been predicted in $CoFe_2O_4$/PZN-PT.[29]

In summary, we have carried out a first-principles study of the interfacial magnetoelectric coupling in tricomponent FM/FE/NM superlattices. Through a detailed analysis of the magnetic moment changes in Fe we have identified the major contributions to the interfacial magnetization. First of all, even in the absence of the FE polarization, the magnetic moment in Fe is significantly reduced by charge transfer from Fe to the oxide owing both to the Fe-O bond formation and metal induced gap states in the oxide. The latter effect is somewhat exacerbated by the underestimated LDA band gap, that can be corrected at e.g., the LDA+U level. Importantly, our LDA+U calculations show that once the FE polarization is turned on the difference between the magnetic moments for two opposite FE polarizations is not sensitive to the band gap. The polarization-induced change in the magnetization at the interface has two separate contributions. We identify a "chemical" contribution that is asymmetric in FE polarization owing to the difference in the interfacial atomic geometry, and thus is interface specific, and the symmetric contribution arising from the spin-dependent screening. The last effect is electrically controllable, linear in the FE polarization, and leads to a substantial magnetoelectric coupling.

This work is supported by the Office of Naval Research under Grant No. N000 14-06-1-0362, NSF under Grant No. DMR-Career-0548182. The authors acknowledge the Texas Advanced Computing Center (TACC) at the University of Texas at Austin for high performance computing resources. Q.N. was supported by (DE-FG02-02ER45958, Division of Materials Science snd Engineering), and the Welch Foundation F-1255. T. C. was supported by NSF (Grant No. DMR0906025), and the Texas Advanced Research Program.

*nsai@physics.utexas.edu
†demkov@physics.utexas.edu

[1] W. Eerenstein, N. D. Mathur, and J. F. Scott, Nature (London) **442**, 759 (2006).
[2] R. Ramesh and N. A. Spaldin, Nature Mater. **6**, 21 (2007).
[3] S.-W. Cheong and M. Mostovoy, Nature Mater. **6**, 13 (2007).
[4] J. F. Scott, Science **315**, 954 (2007).
[5] S. F. Zhang, Phys. Rev. Lett. **83**, 640 (1999).
[6] J. M. Rondinelli, M. Stengel, and N. A. Spaldin, Nat. Nanotechnol. **3**, 46 (2008).
[7] C. G. Duan, S. S. Jaswal, and E. Y. Tsymbal, Phys. Rev. Lett. **97**, 047201 (2006).
[8] T. Y. Cai, S. Ju, J. K. Lee, N. Sai, A. A. Demkov, Q. Niu, Z. Y. Li, J. R. Shi, and E. G. Wang, Phys. Rev. B **80**, 140415(R) (2009).
[9] C. G. Duan, J. P. Velev, R. F. Saviririanov, Z. Q. Zhu, J. H. Chu, S. S. Jaswal, and E. Y. Tsymbal, Phys. Rev. Lett. **101**, 137201 (2008).
[10] M. K. Niranjan, J. P. Velev, C. G. Duan, S. S. Jaswal, and E. Y. Tsymbal, Phys. Rev. B **78**, 104405 (2008).
[11] M. K. Niranjan, J. D. Burton, J. P. Velev, S. S. Jaswal, and E. Y. Tsymbal, Appl. Phys. Lett. **95**, 052501 (2009).
[12] M. Fechner, I. V. Maznichenko, S. Ostanin, A. Ernst, J. Henk, P. Bruno, and I. Mertig, Phys. Rev. B **78**, 212406 (2008).
[13] H. Zheng, J. Wang, S. E. Lofland, Z. Ma, L. Mohaddes-Ardabili, T. Zhao, L. Salamanca-Riba, S. R. Shinde, S. B. Ogale, F. Bai, D. Viehland, Y. Jia, D. G. Schlom, M. Wuttig, A. Roytburd, and R. Ramesh, Science **303**, 661 (2004).
[14] F. Zavaliche, H. Zheng, L. Mohaddes-Ardabili, S. Y. Yang, Q. Zhan, P. Shafer, E. Reilly, R. Chopdekar, Y. Jia, P. Wright, D. G. Schlom, Y. Suzuki, and R. Ramesh, Nano Lett. **5**, 1793 (2005).
[15] G. Kresse and J. Futhmüller, Comput. Mater. Sci. **6**, 15 (1996); Phys. Rev. B **54**, 11169 (1996).
[16] T. Mitsui, M. Adachi, J. Harada, T. Ikeda, S. Nomura, E. Sawguchi, and T. Yamada, *Landolt-Börnstein: Numerical Data and Functional Relationships in Science and Technology*-New Series, Group III, Vol. 16, Pt. 1A (Springer-Verlag, Berlin, 1981).
[17] G. Gerra, A. K. Tagantsev, and N. Setter, Phys. Rev. Lett. **98**, 207601 (2007).
[18] Imposing the tetragonal FE phase ensures that the polarization points perpendicular to the interface. Similar stress-free boundary conditions have been used previously to investigate out-of-plane polarizations in FE thin films (Refs. 30 and 31).
[19] The elastic strain exerted upon Fe due to the lattice mismatch with PTO yields only a 0.7% increase in Fe bulk magnetization.
[20] R. R. Mehta, B. D. Silverman, and J. T. Jacobs, J. Appl. Phys. **44**, 3379 (1973).
[21] N. A. Pertsev and H. Kohlstedt, Phys. Rev. Lett. **98**, 257603 (2007).
[22] P. Ghosez and J. Junquera, *Handbook of theoretical and computational nanotechnology*, edited by M. Reith and W. Schommers, Vol. 9, American Scientific Publishers, CA, 1981), pp. 623.
[23] The metal slabs on both sides are chosen much thicker than the screening length, as indicated by the zero electric field across the central region of the metal electrodes.
[24] W. Zhong, R. D. King-Smith and D. Vanderbilt, Phys. Rev. Lett. **72**, 3618 (1994).
[25] N. Sai, A. M. Kolpak, and A. M. Rappe, Phys. Rev. B **72**, 020101 (2005).
[26] J. K. Lee and A. A. Demkov, Phys. Rev. B **78**, 193104 (2008).
[27] J. Friedel, Nuovo Cimento, Suppl. **7**, 287 (1958).
[28] M. Stengel, D. Vanderbilt, and N. Spaldin, Nature Mater. **8**, 392 (2009).
[29] N. A. Pertsev, Phys. Rev. B **78**, 212102 (2008).
[30] P. Ghosez and K. M. Rabe, Appl. Phys. Lett. **76**, 2767 (2000).
[31] B. Meyer and D. Vanderbilt, Phys. Rev. B **63**, 205426 (2001).